

**United States
Department of
Agriculture**

**Natural Resources
Conservation
Service**

**5 Radnor Corporate Center,
Suite 200
Radnor, PA 19087-4585**

Subject: SOI -- Geophysical Assistance --

Date: 6 June 1996

To: Robert L. Eddleman
State Conservationist
NRCS, Indianapolis, Indiana

Purpose:

The purpose of this investigation was to provide electromagnetic induction (EMI) and ground-penetrating radar (GPR) assistance to the Wet Soil Monitoring Project in Jasper and Jennings counties.

Participants:

Ellis Benham, Research Soil Scientist, USDA-NRCS, Lincoln, NE
Asghar Chowdhery, Soil Scientist, USDA-NRCS, Indianapolis, IN
Jim Doolittle, Research Soil Scientist, USDA-NRCS, Radnor, PA
Don Franzmeier, Professor, Purdue U., Lafayette, IN
Franklin Furr, Soil Scientist, USDA-NRCS, Winamac, IN
Scott Haley, Soil Scientist, USDA-NRCS, Indianapolis, IN
Bill Hostetler, Soil Scientist, USDA-NRCS, Indianapolis, IN
Byron Jenkinson, Research Assistant, Purdue U., Lafayette, IN
Jerry Larson, Soil Scientist, USDA-NRCS, Indianapolis, IN
Dena Marshall, Soil Scientist, USDA-NRCS, North Vernon, IN
Shane McBurnett, Soil Scientist, USDA-NRCS, Winamac, IN
Byron Nagel, Soil Scientist, USDA-NRCS, Indianapolis, IN
Phil Schoeneberger, Research Soil Scientist, USDA-NRCS, Lincoln, NE
Jerry Shively, Soil Scientist, USDA-NRCS, Greencastle, IN
David Tuszyński, ISDH, Indianapolis, IN
Tom Ziegler, Soil Scientist, USDA-NRCS, Indianapolis, IN

Activities:

All field activities were completed during the period of 22 to 25 April 1996. On 22 to 24 April, ground-penetrating radar (GPR) and electromagnetic induction (EMI) field investigations were conducted at the Jasper - Pulaski State Game Preserve. The Preserve is located near the town of San Pierre in Jasper County. On 25 April, electromagnetic induction field investigations were conducted at the Muscatatuck National Wildlife Refuge. The Refuge is located near the town of Hayden in Jennings County.

Equipment:

The radar unit used in this study was the Subsurface Interface Radar (SIR) System-2, manufactured by Geophysical Survey Systems, Inc. The SIR System-2 consists of a digital control unit (DC-2) with

keypad, VGA video screen, and connector panel. The model 3110 (120 mHz) antenna was used in the investigation. The system was powered by a 12-VDC battery. This unit is backpack portable and requires two people to operate. The use and operation of GPR have been discussed by Morey (1974), Doolittle (1987), and Daniels and others (1988).

The electromagnetic induction meters used in this study were the EM38 and EM31, manufactured by Geonics Limited. These meters are portable and require only one person to operate. Principles of operation have been described by McNeill (1980, 1986). No ground contact is required with these meters. Each meter provides limited vertical resolution and depth information. For each meter, lateral resolution is approximately equal to the intercoil spacing. The observation depth of an EMI meter is dependent upon intercoil spacing, transmission frequency, and coil orientation relative to the ground surface.

The EM38 meter has a fixed intercoil spacing of about 1 meter. It operates at a frequency of 13.2 kHz. The EM38 meter has effective observation depths of about 75 and 150 centimeters in the horizontal and vertical dipole orientations, respectively (McNeill, 1986). The EM31 meter has a fixed intercoil spacing of about 3.65 meters. It operates at a frequency of 9.8 kHz. The EM31 meter has effective observation depths of about 3 and 6 meters in the horizontal and vertical dipole orientations, respectively (McNeill, 1980). Values of apparent conductivity are expressed in milliSiemens per meter (mS/m).

A Rockwell Precision Lightweight GPS Receiver (PLGR) was used to obtain the coordinates of observation points. This receiver was operated using an external power source (portable 9 volt battery). During field work, the system was operated in the continuous mode. This mode uses the most power, but is able to acquire and continuously track satellites. Changes in position were continuously displayed. Positions were recorded using the Universal Transverse Mercator (UTM) coordinate system. All recorded points had a *figure of magnitude* (FOM) of 1.

Prior to field work, a digital elevation model (DEM) of the San Pierre Quadrangle was prepared. The DEM data was compiled in 1-degree units. Data consist of a regular array of elevations arranged horizontally using the coordinate system of the World Geodetic System 1972 Datum. Spacing among observations is 3 arc seconds. Data have an absolute horizontal accuracy of 130 meters. Data were compiled in a grid format using the Terrain Analysis Package (TAPPS) developed by Softwright (Golden, Colorado).

A DEM of the Jasper County study site was prepared from elevation data collected at 500 observation points. A theodolite was used to obtain this data. All points were tied into a geodetic survey marker. A 3-meter grid (243 rows by 260 columns) was constructed from this data using the SURFER for Windows program, developed by Golden Software, Inc. Grids were created using kriging methods.

To help summarize the results of this study, the SURFER for Windows program was used to construct two-dimensional simulations. Grids were created using kriging methods with an octant search. All grids were smoothed using a cubic spline interpolation. In each of the enclosed plots, to help emphasize spatial patterns, colors and filled contour lines have been used. Other than showing trends and patterns in values of apparent conductivity (i.e., zones of higher or lower electrical conductivity) or estimated depth to water table, no significance should be attached to the colors themselves.

Discussion:

Jasper County Site:

Background

Recent interest in hydrologic modeling has increased the need for data on the depth and movement of groundwater across landscapes. Presently, much of this information is collected and monitored in wells

and piezometers. By recording the water levels in wells or piezometers, depths to the water table are determined and potentiometric maps prepared. Potentiometric maps are used to estimate ground-water flow direction, flow velocities, and the location of discharge and recharge areas (Freeze and Cherry, 1979).

Typically, potentiometric maps are prepared from data collected from a few, widely spaced monitoring sites. These monitoring sites provide information concerning soil and hydrogeologic conditions at specific locations. However, hydrologic conditions for the large areas among monitoring sites must be inferred. Inferences are often based on simplified assumptions concerning soil and hydrogeologic conditions existing among monitoring sites (Koerner and others, 1979; Violette, 1987).

Toth (1963) defined three categories of groundwater flow: local, intermediate, and regional. In relatively level areas containing homogeneous soil and geologic strata, hydrologic conditions are often relatively uniform and predictable, and groundwater flow conforms to intermediate and regional models. In more sloping area, topography creates numerous subsystems of local groundwater flow within intermediate and regional flow systems (Freeze and Cherry, 1979).

In areas of intricate and contrasting soil patterns, undulating topography, and non-homogeneous or anisotropic materials, depth to the water table and flow patterns are difficult to assess and hydrogeologic data, models, and maps are often oversimplified and susceptible to errors. More comprehensive methods are needed to understand the depth, flow, and seasonal variations of the water table across complex landscapes.

In areas of coarse-textured materials, ground-penetrating radar (GPR) techniques have been successfully used to infer water table depths among monitoring sites and into nearby areas. In areas of coarse-textured materials, GPR techniques can provide continuous records charting the depths to the water table. This geophysical tool can also provide subsurface stratigraphic information useful for hydrologic modeling. In these areas, GPR techniques can be used to increase the quantity and quality of subsurface data, and reduce the need for a large number of monitoring sites.

Ground-penetrating radar techniques have been used to provided data for hydrogeologic models (Violette, 1987; Taylor and Baker, 1988); develop maps of the water table (Sellmann and others, 1983; Davis and others, 1984; Wright and others, 1984; Johnson, 1987; Bohling and others, 1989; Iivari and Doolittle, 1994); define recharge and discharge areas, or the geometry of aquifers (Johnson, 1987; Wright and others, 1984); and delineate near-surface geologic conditions (Beres and Haeni, 1991). Ground-penetrating radar profiles have been used to predict ground-water flow patterns in stratified, coarse-textured soils and to construct three-dimensional computer simulations showing the configuration of soil horizons and geologic strata (Collins and Doolittle, 1987; Steenhuis and others, 1990; Iivari and Doolittle, 1994). In addition, GPR techniques have been used to detect wetting fronts (Vellidis and others, 1989) and contaminant plumes (Horton and others, 1981; Olhoeft, 1986; Cosgrave and others, 1987; Brune and Doolittle, 1990) in sandy soils and to estimate the moisture content of soils (Houck, 1982).

This study is similar to the study conducted by Iivari and Doolittle (1994). In the study by Iivari and Doolittle a map of the water table was developed for an area (3.2 ha.) of glacial-fluvial deposits. The site had moderate relief (about 4 m) and was in hay land. The present study was conducted on a larger (32.8 ha.), more inaccessible, area of eolian deposits. The site had greater relief (about 9.7 m) and was forested. Both studies attempted to demonstrate the feasibility of using GPR and computer processing techniques to chart the depth to the water table and assess local ground water flow in areas having intricate soil patterns, undulating topography, and non-homogeneous or anisotropic strata. The present study attempted to integrate conventional, GPR, and GPS data collection techniques with computer

processing techniques and digital elevation models to map water table depths across relatively large and inaccessible areas.

Study Area:

The study site was located on the San Pierre Quadrangle, Indiana (7.5 minute series). Figure 1 shows the approximate location of the quadrangle in northwestern Indiana and its relationship to the surrounding counties. The site was located in a dune-interdune landscape within the Kankakee outwash plain. The outwash plain has a nearly level topography with low sand dunes or ridges. Sand dunes and ridges have relief as great as 9 meters. The larger dune fields are composed of a series of sand ridges oriented in a northeast - southwest direction. Figure 2 is a three-dimensional surface net diagram of the San Pierre Quadrangle showing the general location of the study site (enclosed rectangle) and its relationship to the Kankakee River, several terraces, and the dune field (hummocky areas to the South of the river). Figure 3 is a three-dimensional surface net diagram of the area surrounding the survey site (enclosed in rectangle). Data points were compiled from a 1-degree unit DEM model. Spacing among observations is 3 arc seconds. The absolute horizontal accuracy of the data is about 130 meters. It became evident that the data points were too few and widely spaced to provide greater resolution of dunes and other features within the study site.

The site was located in the northern half of Section 10, T. 31 N., R. 5 W. The site was in woodland. Twenty-four monitoring wells had been installed across the site. Map units delineated within this area include Oakville fine sands, 2 to 6 percent slopes; Oakville fine sands, 6 to 15 percent slopes; Morocco loamy sands; Newton loamy fine sand, undrained; and Zadog-Maumee loamy sands (Smallwood and Osterholz, 1990). Oakville soils are members of the mixed, mesic Typic Udipsamments family. Morocco soils are members of the mixed, mesic Aquic Udipsamments family. Newton soils are members of the sandy, mixed, mesic Typic Humaquepts family. Maumee soils are members of the sandy, mixed, mesic Typic Haplaquolls family. Zadog soils are members of the coarse-loamy, mixed, mesic Typic Haplaquolls family.

Field Procedures:

The initial GPR survey was conducted along three north - south and three east - west trending access roads. These traverses were completed with the GPR control unit mounted in a vehicle. The 120 mHz antenna was towed behind the vehicle. Three additional lines were established across the southern portion of the study area. These lines were oriented in an east - west direction and spaced about 100 meters apart. As these traverses were conducted through a wooded area, radar traverses were completed with the GPR control unit carried in a backpack and the antenna pulled by hand.

Because of unequal spacing and sampling, only the southern portion of the survey area is evaluated and discussed in this report. This portion of the survey area was more intensively and uniformly sampled with GPR. A survey grid was established across this portion of the site. The grid was composed of five, parallel, west - east trending lines. These lines extended eastwards from a north - south trending base line road (about 330 m). The base line and two additional lines (parallel to the base line) were established on three north - south trending access roads. Each of these lines was about 330 meters in length. Each of the five, west - east lines was about 830 meters in length and spaced about 100 meters apart. Observation flags (178) were inserted along each line at an interval of about 30.5 meters. In addition, a diagonal line was laid out connecting twelve observation wells.

The coordinates of each observation points (178) were obtained with a GPS receiver. The locations of these points are shown in Figure 4. Most of the observation points appear properly spaced, aligned, and correctly oriented. However, slight spatial inaccuracies were presumed to occur in the data. Also shown in Figure 4 are the locations of the monitoring wells used to model water table depths and to correlate the radar imagery.

Prior to this investigation, Byron Jenkinson had completed the topographic mapping of the study area with a theodolite. This survey collected approximately 500 points. This topographic data set was kriged using SURFER for Windows software to produce a grid of the survey area (243 rows by 260 columns)

with a 3 meter interval. Figure 5 is a two-dimensional contour plot of the study site. This plot was prepared from the data collected by Byron Jenkinson. In this plot, the contour interval is 0.5 meter. The site consists of two dunes or ridges separated by a lower-lying inter-dune area. Relief is about 9 meters. In Figure 5, the locations of the 12 monitoring wells used to verify the radar interpretations and to scale the radar imagery are also shown.

The topographic data, radar data, and GPS coordinates were used to construct two- and three-dimensional plots of the study site. These data sets were collected at different times and by different individuals. A concern and source of error were the registering of these data sets. Some information was not directly available and was interpolated. While considered slight, spatial discrepancies undoubtedly occur among the topographic and radar data collected for each observation point. These spatial discrepancies are sources of errors.

The radar survey was completed by pulling the 120 mHz antenna along nine survey lines. This procedure provided about 5840 meters of continuous radar imagery. However, interpretations were restricted to the 178 observation points

Twelve monitoring wells (see Figure 4) had been previously installed within the study site to determine depths to the water table and the directions of ground-water flow. Water levels in the twelve observation wells were measured at the time of the radar survey. These data were used to scale the radar profiles and to construct two-dimensional plots of the water table. The elevation of the water table was determined at each observation point by subtracting the interpreted depth to the water table from the interpolated elevation of the ground surface.

Calibration:

The suitability of using GPR techniques in this terrain was assessed during field trials. These trials established the approximate depth of observation and resolution of the 120 mHz antenna. A scanning time of 160 nanoseconds (ns) and a scan rate of 32.0 scan/second were used in these trials and in all subsequent field work. During these trials, control and recording settings were optimized.

Following calibration, a radar traverse was conducted along a line of fourteen monitoring wells. As the antenna was pulled passed each monitoring well or between each well set, the operator impressed a vertical line on the radar profile (see Figure 6). The GPR is a time scaled system and measures the time that it takes for electromagnetic energy to travel from the antenna to an interface (e.g., water table) and back. In order to convert travel time into a depth scale, the depth to the water table at each observation well was measured and these depths were used to scale the radar imagery. These data were used to determine the dielectric constant and velocity of propagation of electromagnetic energy through the coarse-textured materials. This information was used to construct a crude depth scale for the radar profiles.

For each of the monitoring well, the measured depths to the water table and the interpreted pulse travel time to the water table interface were compared. The coefficient of determination (r^2) between the measured depth and interpreted depth (depth = speed * time) to this interface was 0.9989. The correlation between observation well data and radar interpretations of the depths to the water table was exceptional and exceeds those obtained by Johnson (1987) and Iivari and Doolittle (1994).

The dielectric constant was estimated to be 5.72. Based on the averaged round-trip travel time to the water table the velocity of propagation through the unsaturated, coarse-textured materials was estimated to be 0.038 m/ns. The maximum depth of observation was estimated by the equation:

$$D = VT/2$$

Where D is the depth of observation, V is the velocity of propagation, and T is the two-way travel time of a radar pulse. According to this equation and with a scanning time of 160 ns, the maximum observation depth was about 6.1 meters.

Interpretation of radar profiles:

The study site provided a near-ideal setting for data acquisition with GPR. Figure 6 is a representative radar profile from the study area. The horizontal scale represents units of distance traveled along a grid line. The vertical scale is a time or depth scale, which is based on the estimated velocity of propagation. In this figure, the depth of investigation is about 6 meters (see scale along left-hand margin). The vertical lines represent the locations of the monitoring wells. Letters and numbers have been used to identify the monitoring well. The locations of the monitoring wells identified in this profile are indicated by small triangles in Figure 4.

The radar profile appearing in Figure 6 has been processed through RADAN software. Processing was limited to signal stacking, customizing color transforms and tables, and annotations. Arcone (1982) observed that signal stacking reduces incoherent background noise while enhancing the image of the water table. Often, because of noise suppression, stacked traces have considerably more discernible features especially at greater depths. Computer processing of radar imagery is relatively expensive, time consuming, and not justified for all radar surveys (Violette, 1987). However, in some studies, computer processing of radar imagery has enhanced the resolution of subsurface features and reduced interpretation errors and biases.

In Figure 6, the soil surface is represented by the series of dark, closely spaced, horizontal lines that extend across the upper part of the profile. Subsurface reflectors apparent in this figure included the water table (A), stratification within the eolian deposits (B), and a lower-lying, highly contrasting layer (C). Because of the high-amplitude reflections from the lower-lying layer, it is believed to represent a conspicuous change in texture and a lithologic discontinuity.

In Figure 6, the water table is represented by a strong, nearly continuous and horizontal reflection. In coarse-textured materials, the electromagnetic gradient is abrupt and dielectric properties are strongly contrasting between saturated and unsaturated soil materials. Because of these properties, the upper boundary of the water table produces strong reflections and distinct images on most radar profiles (Shih and others, 1986). These authors observed a decrease in the amplitude and resolution of this interface on radar profiles as the amount of fines in the soil increased and the capillary fringe became more diffuse.

In most portions of this profile (Figure 6), the image of the water table consists of three distinct bands. Because of variations in surface elevations, it ranges in depth from about 0.6 to 6 meters. In areas where the water table is close to the soil surface, its reflection is difficult to identify and trace on radar profiles. In some areas, the image of the water table is obscured by near-surface soil horizons or strata within the eolian deposits.

Figure 7 represents a *terrain corrected* version of Figure 6. Terrain correction is a process whereby the surface of the radar profile is adjusted to conform to the ground topography. At each monitoring well, the radar profile has been adjusted to the elevation of the ground surface. In Figure 7, the water table appears to occur at relatively shallow depths in the lower-lying inter-dune area and plunges to greater depths beneath the higher-lying dunes.

At this time of the year, the apparent direction of groundwater flow is from the inter-dune areas towards the dunes. However, this relationship must be tempered by possible observation and interpretation errors. As mentioned earlier, the topographic, radar, and GPS data sets were collected at different times and by different individuals. A source of error was the registering of these data sets. Some information was not directly available and was interpolated. Slight spatial discrepancies exist among these data sets.

Errors also occurred in the interpretation of the radar imagery. Errors in radar depth interpretation were considered small. Errors in the estimation of the depths to the water table can be attributed to (i) variations in the velocity of propagation of the radar signal through the vadose zone, slight spatial discrepancies among the sites of elevation, GPS, and radar measurement, and (iii) indistinct or obscured images of the water table on some portions of radar profiles.

Within the study site, based on interpretations of the radar profiles taken at the 178 observation points, the average depth to the water table was 2.74 meters with a range of 0.65 to 9.79 meters. One-half of the observations had depths to water table between 1.1 and 3.4 meters. Within the study site, based on measurements taken at 14 monitoring wells, the average depth to the water table was 3.05 meters with a range of 1.04 to 9.70 meters. One-half of the observations had depths to water table between 1.18 and 3.7 meters. The similarity between these two data sets was most remarkable and unexpected. The significance of these data sets may lie with the placement of the monitoring wells and their representation of the larger area.

Computer simulated plots:

Figure 8 is a two-dimensional plot simulating the depth to the water table within the survey site. This simulation is based upon radar interpretations made at 178 observation points. Depths to the water table are variable and closely mimic the topography (see Figure 5) of the survey site. In Figure 8, the locations of the 12 monitoring wells are also shown.

The elevation and relative subsurface topography of the water table have been simulated in Figure 9 and 10. Figure 9 is based on observations made at the twelve monitoring wells. In this plot, the water table appears fairly level across the site. The range in the depths to water table is 1.2 meters. In Figure 9, the direction of flow appears to be towards the left-hand margin. A slight, but noticeable rise in the water table occurs in the lower right-hand corner of this figure.

Figure 10 is based on observations made at the 178 observation points. The larger data base used in this plot has resulted in a more intricate local pattern of ground water relief and flow. In this plot, the range in depths to the water table is 9.14 meters. In this plot, the water table appears fairly level across the inter-dune areas. Conspicuous depressions in the subsurface topography of the water table appear beneath the two higher-lying dunes (compare with Figure 5). However, the locations of these depressions do not correspond with the highest-lying portions of the dunes. The orientations of these depressions appear to be at an angle to the orientation of the ridge lines.

Figure 11 contains a three-dimensional surface net of the surface (upper plot) and the water table (lower plot) within the study site. The topography of the water table conforms to the general form of the land surface. However, several subdued, northwest to southeast trending troughs are evident in the subsurface topography of water table. The reason for these troughs is unclear and it is not known whether these features are real or are artifacts of the survey design.

Jennings County Site:

Study Area:

Study site was located in the Muscatatuck National Wildlife Refuge. The site was located principally in the northwest quarter of Section 19, T. 6 N., R. 7 E. The site was in woodland. Map units delineated within this area include Avonburg silt loam, 0 to 2 percent slopes; Cincinnati-Rossmoyne silt loams, 4 to 10 percent slopes, eroded; Clermont silt loam; and Wakeland silt loam (Nickell, 1976). Avonburg soils are members of the fine-silty, mixed, mesic Aeric Fragiqualfs family. Cincinnati soils are members of the fine-silty, mixed, mesic Typic Fragiudalfs family. Clermont soils are members of the fine-silty, mixed, mesic Typic Ochraqualfs family. Rossmoyne soils are members of the fine-silty, mixed, mesic Aquic Fragiudalfs family. Wakeland soils are members of the coarse-silty, mixed, nonacid, mesic Aeric Fluvaquents family.

Field Procedures:

Each study site was about acres. Random traverses were conducted across the site. Traverses were conducted in straight lines. Lines were abbreviated by several stream channels and areas of ponded water. At varying intervals along each traverse line, measurements were obtained with the EMI meters and the coordinates of these observation points were obtained from the GPS receiver. The distance between observations and traverse lines were selected by the GPS operator to accommodate the steepness and breaks in topographic slopes. These intervals ranged from about 25 to 300 feet. A total of 146 and 86 observation points was recorded on the upland (site #1) and flood plain (site #2) sites, respectively. The locations of these points within each study site are shown in figures 3 and 4.

At each observation point, measurements were taken with the EM38 and EM31 meters in both the horizontal and vertical dipole orientations. For each measurement, the meter was placed on the ground surface. The coordinates of each observation point were recorded with a Rockwell Precision Lightweight GPS receiver.

EMI Interpretations:

Electromagnetic induction techniques use electromagnetic energy to measure the apparent conductivity of earthen materials. Apparent conductivity is a weighted average conductivity measurement for a column of earthen materials to a specific observation depth. Variations in apparent conductivity are produced by changes in the electrical conductivity of earthen materials. The electrical conductivity of soils is influenced by the (i) volumetric water content, (ii) type and concentration of ions in solution, (iii) temperature and phase of the soil water, and (iv) amount and type of clays in the soil matrix, (McNeill, 1980). The apparent conductivity of soils increases with increases in the exchange capacity, water content, and clay content.

Electromagnetic inductive methods measure vertical and lateral variations in the apparent electrical conductivity of earthen materials. Values of apparent conductivity are seldom diagnostic in themselves, but lateral and vertical variations in these measurements can be used to infer changes in soils and earthen materials. Interpretations of the EMI data are based on the identification of spatial patterns within data sets.

Advantages of EMI methods include speed of operation, flexible observation depths (with commercially available systems from about 2.5 to 200 feet), and moderate resolution of subsurface features. Results of EMI surveys are interpretable in the field. This technique can provide in a relatively short time the large number of observations needed for site characterization and assessments. Maps prepared from correctly interpreted EMI data provide the basis for assessing site conditions and for planning further investigations.

Electromagnetic induction techniques are not suitable for use in all investigations. Generally, the use of EMI techniques has been most successful in areas of undisturbed soils where subsurface properties are reasonably homogeneous, the effects of one property (e.g. clay, water, or salt content) dominates over the other properties, and variations in EMI response can be related to changes in the dominant property (Cook and others, 1989).

Field Procedures:

Random traverses were conducted across the site. The site was wooded and lines were abbreviated and reoriented by several stream channels and wet areas. At varying intervals along each traverse line, measurements were obtained with the EMI meters and the coordinates of these observation points were obtained from the GPS receiver. A total of 41 observation points was recorded on the sites. The locations of these points are shown in Figure.

At each observation point, measurements were taken with the EM38 and EM31 meters in both the horizontal and vertical dipole orientations. For each measurement, the meter was placed on the ground

surface. The coordinates of each observation point were recorded with a Rockwell Precision Lightweight GPS receiver.

Discussion:

Basic statistics for the EMI data collected within the Muscatatuck site are displayed in Table 1. In general, values of apparent conductivity increased and became more variable with increasing observation depths. Values of apparent conductivity increased with increasing observation depths. For the shallower sensing EM38 meter, measurements averaged 7.4 mS/m and 11.2 mS/m in the horizontal and vertical dipole orientations, respectively. One-half of the observations had values of apparent conductivity between 6.0 and 8.3 mS/m in the horizontal (0 to 75 centimeters), and between 10.2 and 12.7 mS/m in the vertical (0 to 150 centimeters) dipole orientation. For the deeper sensing EM31 meter, measurements averaged 20.4 mS/m and 27.8 mS/m in the horizontal and vertical dipole orientations, respectively. One-half of the observations had values of apparent conductivity between 16.4 and 23.3 mS/m in the horizontal (0 to 3 meters), and between 21.6 and 32.4 mS/m in the vertical (0 to 6 meters) dipole orientations.

Table 1
Basic Statistics
EMI Survey
Muscatatuck Site
(All values are in mS/m)

Meter	Orientation	Quartiles					
		Minimum	Maximum	1 st	Median	3rd	Average
EM38	Horizontal	3.6	13.2	6.0	7.4	8.3	7.4
EM38	Vertical	4.9	21.2	10.2	11.6	12.7	11.2
EM31	Horizontal	9.5	33.1	16.4	21.6	23.3	20.4
EM31	Vertical	12.4	45.3	21.6	29.2	32.4	27.8

Figures 6 and 7 are two-dimensional plots of data collected with the EM38 meter in the horizontal and vertical dipole orientations, respectively. Figures 8 and 9 are two-dimensional plots of data collected with the EM31 meter in the horizontal and vertical dipole orientations, respectively. In each of these plots, the isoline interval is 2 mS/m.

With kind regards,

James A. Doolittle
Research Soil Scientist

cc:

J. Culver, Supervisory Soil Scientist, USDA-NRCS, National Soil Survey Center, Federal Building,
Room 152, 100 Centennial Mall North, Lincoln, NE 68508-3866

W. Hostetler, Assistant State Soil Scientist, USDA-NRCS, RR #2, Box 90, Frankfort, IN 46041

S. Holzhey, Supervisory Soil Scientist, USDA-NRCS, National Soil Survey Center, Federal Building,
Room 152, 100 Centennial Mall North, Lincoln, NE 68508-3866

B. Jenkinson, Graduate Student, Agronomy Department, Purdue University, West Lafayette, IN 47907

T. Neely, State Soil Scientist/MO Leader, USDA-NRCS, Indianapolis, IN

References

- Arcone, S. 1982. Radar detection of ground water. p. 68-76. IN: Dardeau, E. A. (ed.) Proceedings of the Ground-Water Detection Workshop. 12-14 January 1982. Vicksburg, Mississippi. Department of the Army. Waterways Experiment Station.
- Beres, M. and F. P. Haeni. 1991. Application of ground-penetrating radar methods in hydrogeologic studies. *Ground Water* 29(3):375-386.
- Bohling, G. C., M. P. Anderson, C. R. Bentley. 1989. Use of ground penetrating radar to define recharge areas in the Central Sand Plain. Technical Completion Report G1458-03. Geology and Geophysics Department, University of Wisconsin-Madison. 62 pp.
- Brune, D. E., and J. Doolittle 1990. Locating lagoon seepage with radar and electromagnetic survey. *Environ. Geol. Water Sci.* 16(3):195-207.
- Collins, M. E. and J. A. Doolittle. 1987. Using ground-penetrating radar to study soil microvariability. *Soil Science Society of America J.* 51: 491-493.
- Cook, P. G., M. W. Hughes, G. R. Walker, and G. B. Allison. 1989. The calibration of frequency-domain electromagnetic induction meters and their possible use in recharge studies. *Journal of Hydrology* 107:251-265.
- Cosgrave, T. M., J. P. Greenhouse, and J. F. Barker. 1987. Shallow stratigraphic reflections from ground-penetrating radar. p. 555-569. IN: Proceeding of First National Outdoor Action Conference on Aquifer Restoration, Ground Water Monitoring and Geophysical Methods. May 18-21, 1987. Las Vegas, Nevada. National Water Well Association, Dublin, Ohio.
- Davis, J. L., R. W. D. Killey, A. P. Annan, and C. Vaughan. 1984. Surface and borehole ground-penetrating radar surveys for mapping geologic structures. Proceedings of the National Water Well Association/Environmental Protection Agency Conference on Surface and Borehole Geophysical Methods in Ground Water Investigations. Feb. 7-9, 1984. San Antonio, Texas. p. 681-712.
- Daniels, D. J., D. J. Gunton, and H. F. Scott. 1988. Introduction to subsurface radar. *IEE Proceedings* 135F (4):278-320.
- Doolittle, J. A. 1987. Using ground-penetrating radar to increase the quality and efficiency of soil surveys. IN *Soil Survey Techniques*, Soil Science Society of America Special Publ. No 20. pp. 11-32.
- Freeze, R. A., and J. A. Cherry. 1979. *Groundwater*. Prentice-Hall, Inc. Englewood Cliffs, New Jersey. pp. 604.
- Houck, R. T. 1982. Measuring moisture content profiles using ground-probing radar. Technical Report, XADAR Corporation, Springfield, Virginia. pp. 1-10.
- Horton, K. A., R. Morey, R. H. Beers, V. Jordan, S. S. Sandler, and L. Isaacson. 1981. An evaluation of ground-penetrating radar for assessment of low level nuclear waste disposal sites. Office of Nuclear Regulatory Research. Nuclear Regulatory Commission, Report Number NUREG/CR2212.
- Iivari, T. A. and J. A. Doolittle. 1994. Computer simulations of depths to water table using ground-penetrating radar in topographically diverse terrains. pp. 11-20. IN: Kovar, K. and J. Soveri (eds.).

Groundwater Quality Management (Proceedings of GQM 93, International Association of Hydrological Sciences. Conference held at Tallinn, Estonia. September 1993. p. 485.

Johnson, D. G. 1987. Use of ground-penetrating radar for determining depth to the water table on Cape Cod, Massachusetts. p. 541-554. *IN*: Proceeding of First National Outdoor Action Conference on Aquifer Restoration, Ground Water Monitoring and Geophysical Methods. May 18-21, 1987. Las Vegas, Nevada. National Water Well Association, Dublin, Ohio.

Koerner, R. M., J. S. Reif, M. J. Burlingame. 1979. Detection methods for location of subsurface water and seepage. *Journal of the Geotechnical Engineering Division, ASCE*, Vol. 105, No. GT11. pp. 1301-1316.

McNeill, J. D. 1980. Electromagnetic terrain conductivity measurement at low induction numbers. Technical Note TN-6. Geonics Limited, Mississauga, Ontario. 15 p.

McNeill, J. D. 1986. Geonics EM38 ground conductivity meter operating instructions and survey interpretation techniques. Technical Note TN-21. Geonics Ltd., Mississauga, Ontario. pp. 16.

Morey, R. M. 1974. Continuous subsurface profiling by impulse radar. pp. 212-232. *In*: Proceedings, ASCE Engineering Foundation Conference on Subsurface Exploration for Underground Excavations and Heavy Construction, held at Henniker, New Hampshire. Aug. 11-16, 1974.

Nickell, A. E. 1976. Soil Survey of Jennings County, Indiana. USDA-Soil Conservation Service. U. S. Government Printing Office. Washington, D. C. pp. 91.

Olhoeft, G. R. 1986. Direct detection of hydrocarbon and organic chemicals with ground-penetrating radar and complex resistivity. p. 1-22. *IN*: Proceedings of the National Water Well Association Conference on Petroleum Hydrocarbons and Organic Chemicals in Groundwater. Houston, Texas.

Palacky, G. J. and L. E. Stephens. 1990. Mapping of Quaternary sediments in northeastern Ontario using ground electromagnetic methods. *Geophysics* 55:1596-1604.

Sellmann, P. V., S. A. Arcone, A. J. Delaney. 1983. Radar profiling of buried reflectors and the groundwater table. Cold Region Research and Engineering Laboratory Report 83-11. Hanover, New Hampshire. pp. 1-10.

Shih, S. F., J. A. Doolittle, D. L. Myhre, and G. W. Schellentrager. 1986. Using radar for ground water investigation. *Journal of Irrigation and Drainage Engineering* 112(2):110-118.

Smallwood, B. F. and L. C. Osterholz. 1990. Soil Survey of Jasper County, Indiana. USDA-Soil Conservation Service. U. S. Government Printing Office. Washington, D. C. pp. 205.

Steenhuis, T. S., K.-J. S. Kung, and L. M. Cathles III. 1990. Finding layers in the soil. Ground-penetrating radar as a tool in studies of groundwater contamination. *Engineering Cornell Quarterly* (Autumn):15-19.

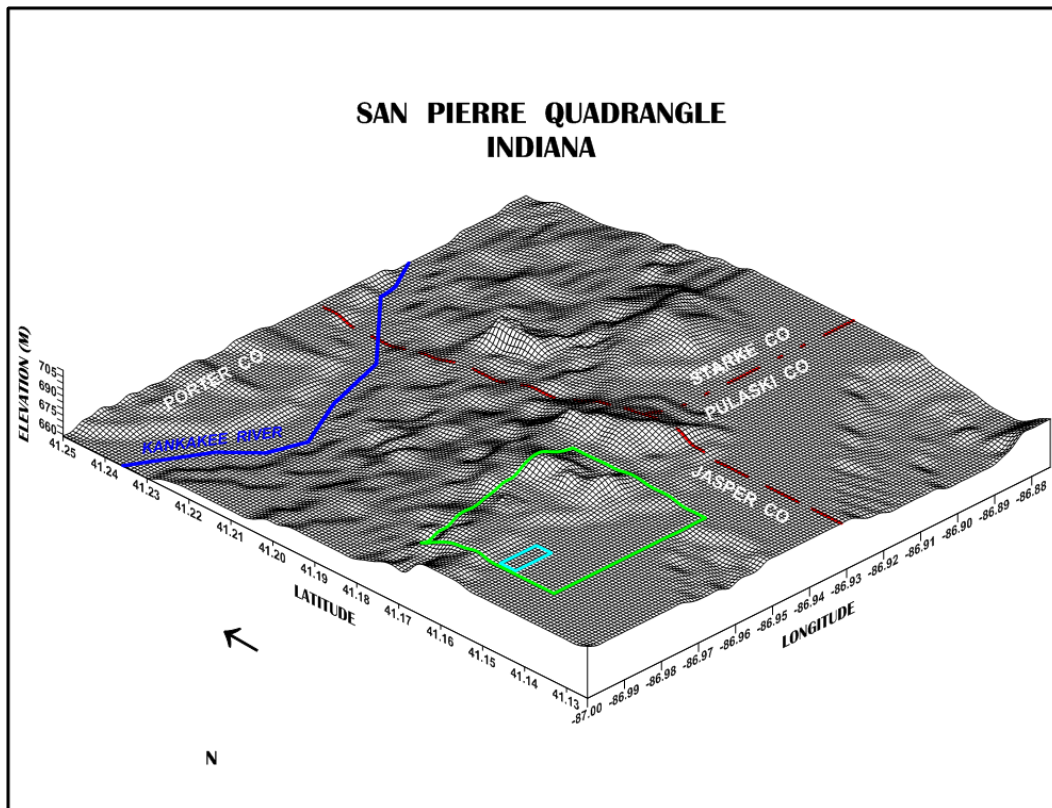
Taylor, K. R. and M. E. Baker. 1988. Use of ground-penetrating radar in defining glacial outwash aquifers. p. 70-98. *IN*: Proceeding of the FOCUS Conference on Eastern Regional Ground Water Issues, Stamford, Connecticut. September 27-29, 1988. National Water Well Association, Dublin, Ohio.

Toth, J. 1963. A theoretical analysis of groundwater flow in small drainage basins. *Journal of Geophysical Research*, 68:4795-4812.

Vellidis, G., M. C. Smith, D. L. Thomas, M. A. Breve, and C. D. Perry. 1989. Using ground-penetrating radar (GPR) to detect soil water movement in sandy soil. American Society of Agricultural Engineers Paper No. 89-2520. St., Joseph, Michigan: ASAE. pp. 13.

Violette, P. 1987. Surface geophysical techniques for aquifers and wellhead protection area delineation. Environmental Protection Agency, Office of Ground Water Protection, Washington, D.C., pp. 1-49.

Wright, D. L., G. R. Olhoeft, and R. D. Watt. 1984. Ground-penetrating radar studies on Cape Cod. p. 666-680. IN: D. M. Neilsen (ed.) Surface and Borehole Geophysical Methods in Ground Water Investigations. National Water Well Association, Worthington, Ohio.



**WET SOIL MONITORING PROJECT
JASPER PULASKI STATE GAME PRESERVE
JASPER COUNTY, INDIANA**

LOCATION OF OBSERVATION AND MONITORY WELL SITES

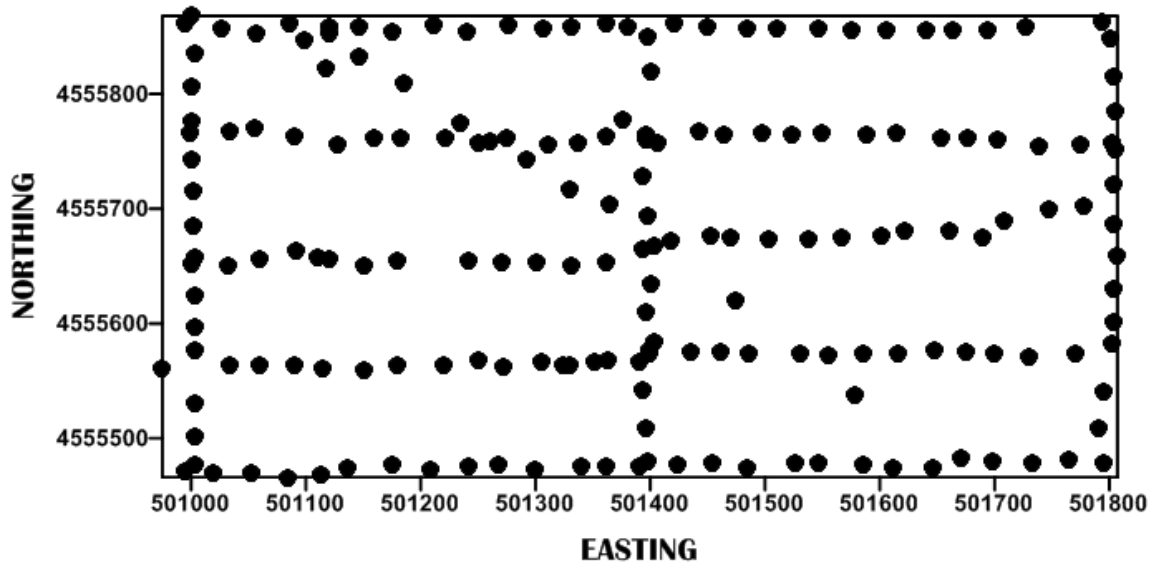


FIGURE 4 ● **OBSERVATION SITE**

**WET SOIL MONITORING PROJECT
JASPER PULASKI STATE GAME PRESERVE
JASPER COUNTY, INDIANA
RELATIVE TOPOGRAPHY
CONTOUR INTERVAL = 0.5 M**

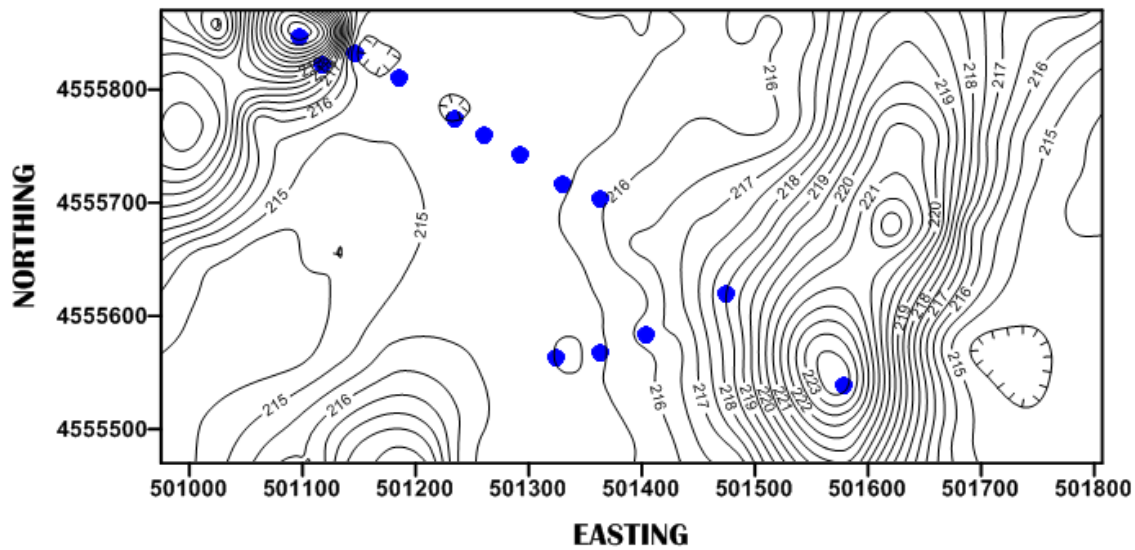


FIGURE 5 ● **MONITORING WELL**

**WET SOIL MONITORING PROJECT
JASPER PULASKI STATE GAME PRESERVE
JASPER COUNTY, INDIANA
DEPTH TO WATER TABLE
INTERVAL = 0.5 M**

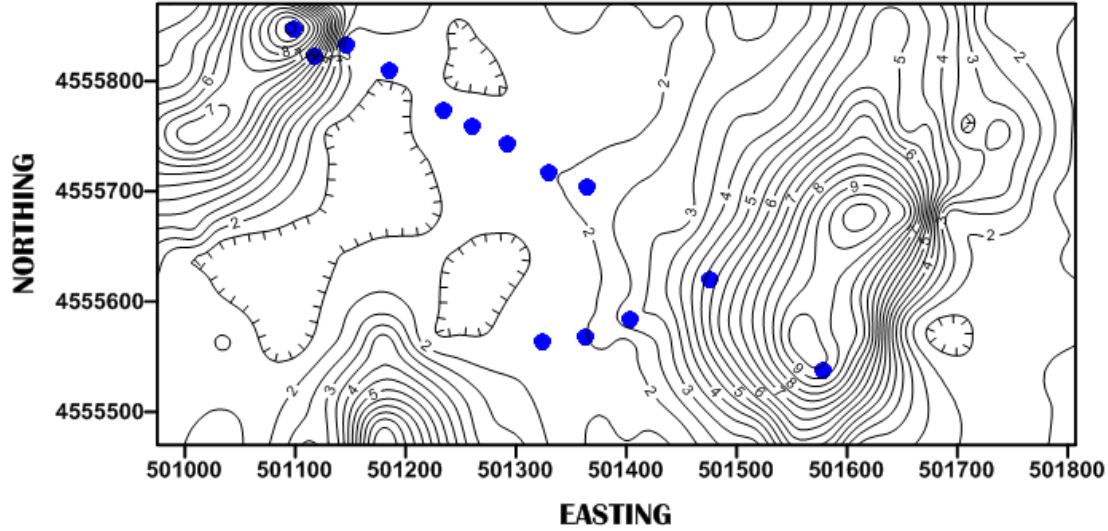


FIGURE 8

● **MONITORING WELL**

**WET SOIL MONITORING PROJECT
JASPER PULASKI STATE GAME PRESERVE
JASPER COUNTY, INDIANA
RELATIVE TOPOGRAPHY OF WATER TABLE
CONTOUR INTERVAL = 0.25 M**

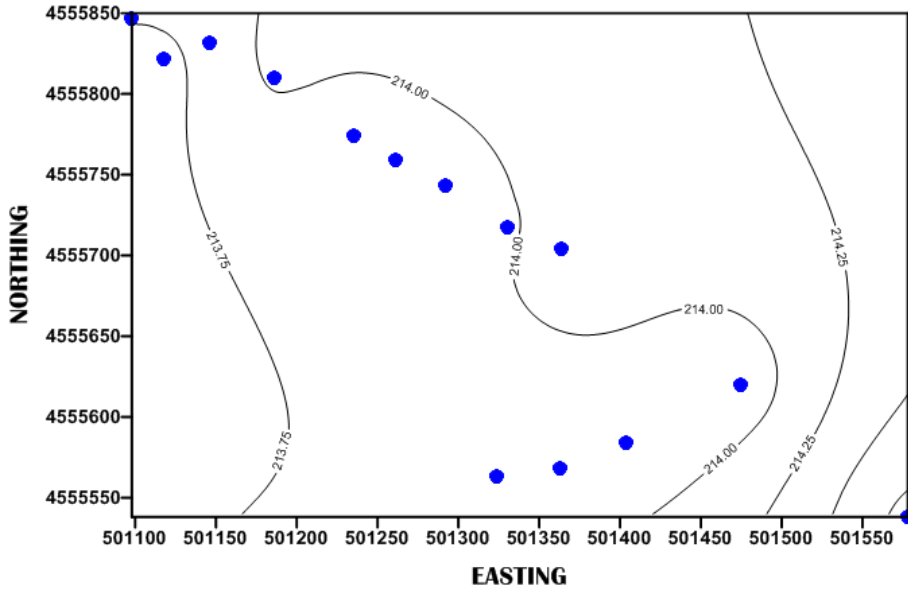


FIGURE 9

● **MONITORING WELL**

**WET SOIL MONITORING PROJECT
JASPER PULASKI STATE GAME PRESERVE
JASPER COUNTY, INDIANA
RELATIVE TOPOGRAPHY OF THE WATER TABLE
INTERVAL = 0.5 M**

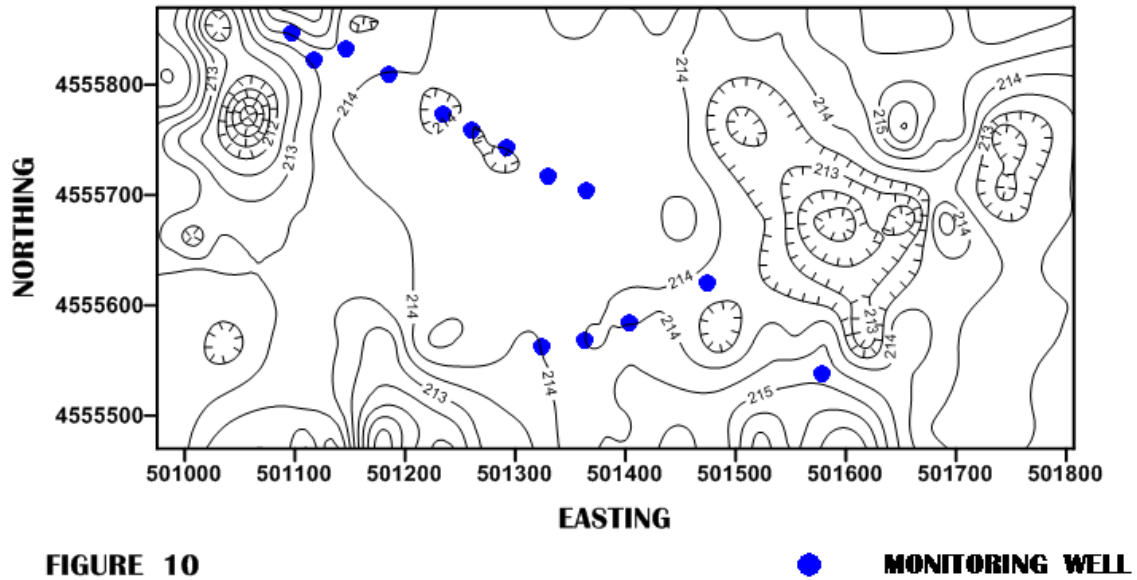


FIGURE 10

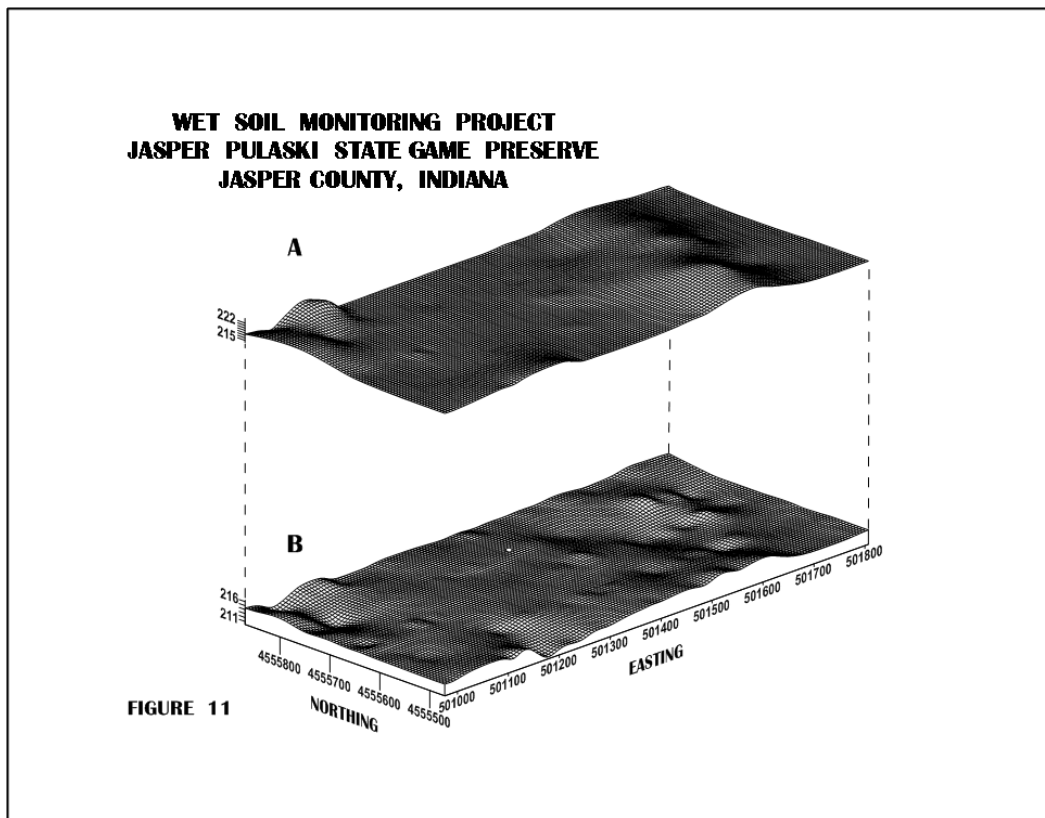
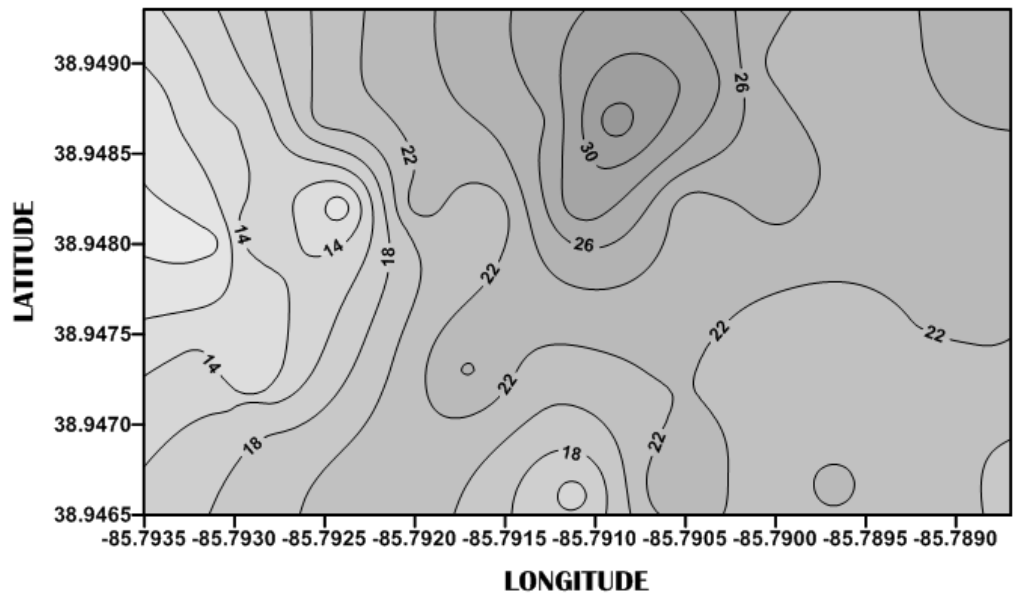


FIGURE 11

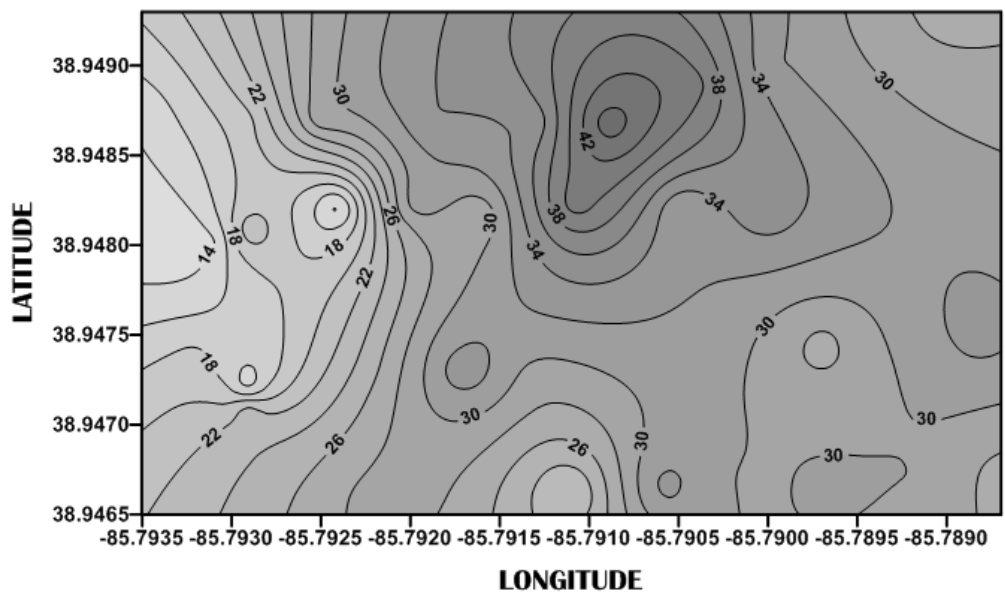
MUSCATATUCK NATIONAL WILDLIFE REFUGE JENNINGS COUNTY, INDIANA

EM SURVEY
EM31 METER
HORIZONTAL DIPOLE ORIENTATION



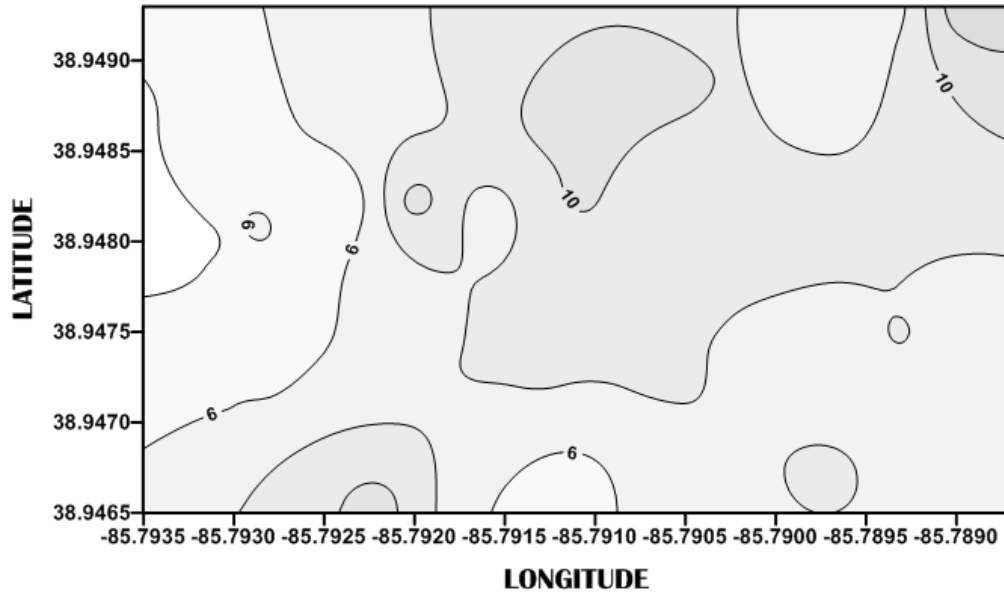
MUSCATATUCK NATIONAL WILDLIFE REFUGE JENNINGS COUNTY, INDIANA

EM SURVEY
EM31 METER
VERTICAL DIPOLE ORIENTATION



MUSCATATUCK NATIONAL WILDLIFE REFUGE JENNINGS COUNTY, INDIANA

EM SURVEY
EM38 METER
HORIZONTAL DIPOLE ORIENTATION



MUSCATATUCK NATIONAL WILDLIFE REFUGE JENNINGS COUNTY, INDIANA

EM SURVEY
EM38 METER
VERTICAL DIPOLE ORIENTATION

